Title

Toxicity of biosynthesized silver nanoparticles to aquatic organisms of different trophic levels

Authors

Khoshnamvand, Mehdi

Hao, Zhineng

Fadare, Oluniyi O

et al.

Publication Date

2020-11-01

DOI

10.1016/j.chemosphere.2020.127346

Chemosphere 258 (2020) 127346

Contents lists available at ScienceDirect

Chemosphere

journal homepage: www.elsevier.com/locate/chemosphere

Toxicity of biosynthesized silver nanoparticles to aquatic organisms of different trophic levels

Mehdi Khoshnamvand [a, b], Zhineng Hao [a], Oluniyi O. Fadare [a, b], Parichehr Hanachi [c], Yongsheng Chen [d], Jingfu Liu [a, e, *]

[a] State Key Laboratory of Environmental Chemistry and Ecotoxicology, Research Center for Eco-Environmental Sciences, Chinese Academy of Sciences, Beijing, 100085, China
[b] University of Chinese Academy of Sciences, Beijing, 100049, China
[c] Department of Biotechnology, Faculty of Biological Science, Alzahra University, Tehran, Iran
[d] School of Civil and Environmental Engineering, Georgia Institute of Technology, Atlanta, GA, 30332, USA
[e] Institute of Environment and Health, Jianghan University, Hubei Province, Wuhan, 430056, China

HIGHLIGHTS

- Using leaf extract of herbal plant *Alcea rosea*, AR-AgNPs were synthesized.
- Coating agents of AR-AgNPs showed no toxicity to organisms of the studied food chain.
- Ag^+ ions were more toxic in comparison to AR-AgNPs at all the three trophic levels.
- Toxicity of AR-AgNPs stemmed mainly from AR-AgNPs rather than Ag^+ ions.

GRAPHICAL ABSTRACT

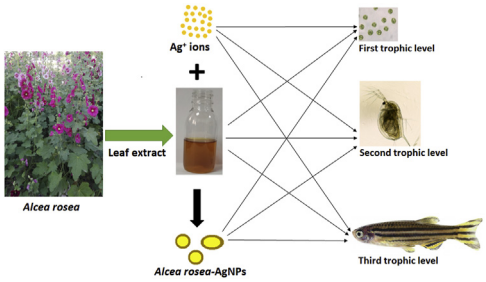

ARTICLE INFO

Article history:
Received 4 April 2020
Received in revised form
29 May 2020
Accepted 5 June 2020
Available online 10 June 2020

Handling Editor: Tamara S. Galloway

Keywords:
Toxicity
Silver nanoparticles
Biosynthesized nanoparticles
Aquatic organisms
Trophic level

ABSTRACT

Although biosynthesized nanoparticles are regarded as green products, research on their toxicity to aquatic food chains is scarce. Herein, biosynthesized silver nanoparticles (*Alcea rosea*-silver nanoparticles, AR-AgNPs) were produced by the reaction of Ag ions with leaf extract of herbal plant *Alcea rosea*. Then, the toxic effects of AR-AgNPs and their precursors such as Ag^+ ions and coating agent (*A. rosea* leaf extract) on organisms of different trophic levels of a freshwater food chain were investigated. To the three studied aquatic organisms including phytoplankton (*Chlorella vulgaris*), zooplankton (*Daphnia magna*) and fish (*Danio rerio*), the coating agents of AR-AgNPs showed no toxic effects, and Ag^+ ions were more toxic in comparison to AR-AgNPs. Further investigations revealed that the release of Ag^+ ions from AR-AgNPs to the test media were not considerable due to the high stability of AR-AgNPs, thus the toxicity stemmed mainly from the particles of AR-AgNPs in all the three trophic levels. Based on values of 72-h EC_{50} for *C. vulgaris*, 48-h LC_{50} for *D. magna* and 96-h LC_{50} for *D. rerio*, the most sensitive organism to AR-AgNPs exposure was *D. magna* (the second trophic level).

* Corresponding author. State Key Laboratory of Environmental Chemistry and Ecotoxicology, Research Center for Eco-Environmental Sciences, 18 Shuangqing Road, Haidian District, Beijing, P. O. Box 2871, 100085, China.
E-mail addresses: mehdi.khoshnam@yahoo.com (M. Khoshnamvand), znhao@rcees.ac.cn (Z. Hao), fadare@rcees.ac.cn (O.O. Fadare), p.hanachi@alzahra.ac.ir (P. Hanachi), yongsheng.chen@ce.gatech.edu (Y. Chen), jfliu@rcees.ac.cn (J. Liu).

https://doi.org/10.1016/j.chemosphere.2020.127346
0045-6535/

1. Introduction

Nanoparticles (NPs) are widely used in various areas including energy, optoelectronics industry, chemical sensors, medical care, environmental protection, agricultural and food productions (Sharma et al., 2015; Khoshnamvand et al., 2020a, 2020b). Thousands of tons of NPs are produced worldwide every year, and it is estimated that the annual output of NPs will be far more than 5 million tons around the world by 2020 (Weinberg et al., 2011), and more than 1800 products containing NPs are in the market (He et al., 2019; Nie et al., 2020). Among them, silver nanoparticles (AgNPs) are employed in various areas like microelectronics, information storage and antimicrobial (Yu et al., 2013), which make their inevitable discharge into the environment accidently or deliberately (He et al., 2015). After entering into the aquatic environments, AgNPs would exert their toxic effects on numerous organisms through different pathways (Khoshnamvand et al., 2020a; Nie et al., 2020). The key to ameliorate adverse impacts of AgNPs to the environment is to avoid the release of AgNPs and develop green synthetic methods in which toxic chemicals are minimally used.

AgNPs can be biosynthesized by using the biological systems such as actinomycetes, yeast, fungi, bacteria, algae and plant at normal temperature and pressure in the absence of toxic materials (Shankar et al., 2016). Although the biosynthesis procedure is green, it is uncertain if the biosynthesized AgNPs is a green product as knowledge on their toxic effects to environment is scarce.

Previous studies have showed that the toxicity of physiochemically synthesized AgNPs depended on some parameters such as the particle size (Shen et al., 2015), coating agent (Sakka et al., 2016), released Ag^+ ions from AgNPs themselves (Shen et al., 2015) and released reactive oxygen species and binding to DNA (Lubick, 2008; Choi et al., 2010; Mulenos et al., 2020). However, these findings are not necessarily applicable to biosynthesized AgNPs due to the differences in coatings. Currently, a few studies evaluated the toxicity of biosynthesized AgNPs to a single aquatic species (Rani and Rajasekharreddy, 2011; Ali et al., 2019; Khoshnamvand et al., 2020a), but there is no detailed study on their toxicity to aquatic organisms of different trophic levels. Therefore, studies on the toxic effects of biosynthesized AgNPs to different organisms are urgently needed.

Various aquatic organisms of different trophic levels have been adopted as models to evaluate the toxicity of different pollutants. *Chlorella vulgaris* is widely used as a model aquatic organism for toxic studies as it multiplies asexually and rapidly in optimum conditions within 24 h (Oukarroum et al., 2012); thus, it was selected as the first tropic level. As a standard species in acute toxicity testing, *Daphnia magna* with characteristics of a short life cycle and sensitive to contaminants (Persoone et al., 2009) was employed as the second tropic level. *Danio rerio* was adopted as the third trophic level as it has similar characteristics of morphology, histology and physiology to the mammals (Howe et al., 2013), and has become a popular laboratory animal model for nanotoxicology researches (Jang et al., 2014).

As an important herbal plant, *Alcea rosea* is traditionally used as diuretic, cooling, emmenagogue and expectorant substance (Ebrahiminezhad et al., 2017; Khoshnamvand et al., 2019a). Some of these characteristics might be inherited by biosynthesis of AgNPs with *A. rosea* (AR-AgNPs), leading to the production of AgNPs with different effects to the environment in comparison to physic-chemically synthesized ones. Hence, in this study, AR-AgNPs were produced by using the aqueous extract of dry leaves of *A. rosea* as reducing and capping agent. Then, the toxic effects of AR-AgNPs and their precursors to different trophic levels of a food chain were studied including microalgae *Chlorella vulgaris*, microcrustacean *Daphnia magna* and zebrafish *Danio rerio*. In addition, the contributions of AR-AgNPs, released free Ag^+ ions from AR-AgNPs, and the coating agent to toxicity were evaluated. The findings of this study provide a better understanding and new insight on potential toxicity risks of biosynthesized AgNPs towards aquatic organisms of different trophic levels.

2. Materials and methods

2.1. Chemicals and materials

Silver nitrate ($AgNO_3 \geq 99.8\%$) was purchased from Sigma-Aldrich (St. Louis, MO, USA) and used without further purification. Other chemicals were obtained from Sinopharm Chemical Reagent Co., Ltd (Shanghai, China). Millipore water was prepared by a Milli-Q Gradient system (Millipore, Bedford, MA, USA) and used throughout the experiments.

2.2. Synthesis of AR-AgNPs

The *A. rosea* was collected from Shahe University Park, Beijing (China). The *A. rosea* leaves were washed with deionized water and dried in air at room temperature, and milled to powder with a grinder. The aqueous leaf extract was prepared by boiling 5 g of fine leaf powder in Millipore water (100 mL) at 60 °C for 30 min. The extract was then carefully filtered using 0.45 μm membrane filters (mixed cellulose esters, Millipore, Billerica, MA, USA). Subsequently, 1 mL of the aqueous extract was added into 60 mL of 1 mM $AgNO_3$ aqueous solution at 60 °C under stirring. With the passing of time, the mixture color altered from colorless to brown, denoting formation of AR-AgNPs.

The yield of AR-AgNPs was determined according to a reported procedure (Yuan et al., 2017). Briefly, Ag(I) ions were separated from AR-AgNPs with an ultrafiltration tube (Amicon Ultra-15, 30 kD, Millipore, MA, USA) conducted at 10000 rpm for 30 min. Subsequently, the unreacted Ag(I) ions in the filtrate were measured by the inductively coupled plasma-mass spectrometer (ICP-MS, Agilent 7700, Santa Clara, CA, USA), and the yield of AR-AgNPs was finally calculated by deducting the remaining Ag(I) ions in the filtrate from the total Ag^+ ions as reactant (1 mM).

2.3. Characterization of AR-AgNPs

Different instruments/techniques such as UV−vis spectrophotometer (UV-3600, Shimadzu, Japan), Zetasizer (Nano-ZS zen 3600, Malvern Instruments, Worcestershire, UK), transmission electron microscopy (TEM, Hitachi H-7500, Japan), scanning electron microscopy (SEM, Hitachi SU8020, Japan), energy-dispersive X-ray spectroscopy (EDX, Hitachi SU8020, Japan), X-ray diffractometer (XRD, X' Pert Pro P Analytical X-ray diffractometer instrument, Almelo, Netherlands) and Fourier transform infrared spectroscopy (FTIR, Nicolet 6700, Madison, WI, USA) were used to characterize the formed AR-AgNPs (see Supplementary Material for details).

2.4. C. vulgaris culture and toxicity tests

C. vulgaris were cultivated in our laboratory. The culture conditions and toxicity tests of algae biomass and chlorophyll *a* were carried out based on the standard of Organization for Economic Cooperation and Development, OECD guideline number of 201 (OECD, 2011; see Supplementary Material).

2.5. D. magna culture and toxicity tests

D. magna originates from Birmingham University (U.K). The culture conditions and acute (48 h) toxicity tests of AR-AgNPs and

their precursors to *D. magna* were conducted according to the *Daphnia* Sp. acute immobilization test (OECD guideline number of 202 (OECD, 2004; see Supplementary Material).

2.6. D. rerio toxicity tests

Adult zebrafish (*D. rerio*) were obtained from China zebrafish resource center (Wuhan). To evaluate the toxic effects of AR-AgNPs, Ag^+ ions and the coating agent of AR-AgNPs to *D. rerio*, the acute (96 h) toxicity tests were carried out based on the OECD guideline number of 203 (OECD, 1992). Moreover, to test the effects of treatments on inhibition of acetylcholinesterase activity, a biomarker of neurotoxicity (Manzo et al., 2001), muscle and gill of *D. rerio* were studied (see Supplementary Material).

2.7. Data analysis

Data were tested using Kolmogorov-Smirnov and Levene's tests for normal distribution and homogeneity of variances, respectively. SPSS software version 16.0 (SPSS Inc., Chicago, IL, USA) was used to analyze the results of experiments which are presented as mean ± standard deviation. The values of 72 h-EC_{50} for *C. vulgaris*, 48-LC_{50} for *D. magna* and 96 h-LC_{50} for *D. rerio* after exposure to corresponding treatments were calculated using the probit analysis in SPSS. In addition, one-way analysis of variance (ANOVA) was used to find differences among exposure groups at similar/different times with a post-hoc Duncan's test, and *P*-values less than 0.05 were considered statistically significant. Nonlinear regression sigmoidal dose-response curves were drawn using Origin software version 2017 (OriginLab Corporation, Northampton, MA, USA), whereas the others were drawn by Microsoft Excel version 2016 (Microsoft Corporation, Redmond, WA, USA).

3. Results and discussion

3.1. Optimization of synthesis conditions

It has been proved that the biomolecules existing in plant extract play an important role in the features of obtained AgNPs (Sanchez et al., 2016). However, the function of other parameters such as temperature, pH, amount of extract and reaction time cannot to be ignored (Sanchez et al., 2016; Ajitha et al., 2015). In this work, different volume (mL) ratios of leaf extract to $AgNO_3$ (1 mM), i.e. 1:30, 1:40, 1:50 and 1:60 were used to evaluate the effect of leaf extract quantity on the AR-AgNPs synthesis (Fig. S1). Dependent on the volume ratio of leaf extract to $AgNO_3$, the surface plasmon resonance (SPR) peaks recorded using UV−vis were between 420 and 460 nm, except for the 1:30 ratio due to high aggregation. The highest and lowest SPR bands were observed at ratios of 1:50 and 1:30, respectively. However, at 24 h after synthesisation, aggregation was observed in all samples except for that with 1:60 ratio. Therefore, this 1:60 ratio was chosen for further studies.

The effect of $AgNO_3$ concentration on synthesis of AR-AgNPs was further investigated. UV−vis recording showed that the AR-AgNPs formed at 4 mM $AgNO_3$ had the highest peak (Fig. S1b), but aggregation occurred for AR-AgNPs synthesized with 2 and 4 mM $AgNO_3$. Therefore, 1 mM $AgNO_3$ was used in this study.

Although the pH of the synthesis reaction is expected to influence the formation of AR-AgNPs, it was not optimized to avoid the use of chemical agents like NaOH or HCl to establish an environmentally friendly biosynthesis procedure. The reaction temperature was set at 60 °C, under which the mixture gradually changed from colorless to brown due to excitation of SPR of the formed AR-AgNPs (Fig. S2). After reaction for 6 h, the mixture color did not change (Fig. S2), suggesting the reach of reaction equilibrium. Thus, a reaction time of 7 h was adopted.

Under the above optimized conditions, approximately 100% of Ag^+ ions were converted into AR-AgNPs. Such very high yield of AR-AgNPs suggested that *A. rosea* leaves have a considerable potential for manufacturing of AR-AgNPs through green synthesis process.

3.2. Characterization of AR-AgNPs

The mean sizes of AR-AgNPs at the start (0 h), 24, 48, 72 and 96 h after synthesis were analyzed by dynamic light scattering (DLS), (Fig. S3), and the mean size of the synthesized AR-AgNPs was 49.05 ± 25.34 nm and finally increased to 76.94 ± 36.82 after 96 h. This indicated an increase trend of hydrodynamic size of the AR-AgNPs during the studied period. In addition, all the zeta potential values of AR-AgNPs collected at different times were negative and the absolute values decreased slightly with the passage of time (Fig. S3), suggesting the electrostatic repulsion between AR-AgNPs, and thus, stability of NPs (Khoshnamvand et al., 2019b).

Fig. 1a and Fig. 1b show the TEM and SEM analyses of the prepared AR-AgNPs, which were polydispersed particles with spherical and quasi-spherical shapes, and had high density and regular dispersity. EDX analysis indicates the presence of elemental Ag peaks ranged from 2 to 4 keV (Fig. S4). The intense peak at around 1.7 keV corresponds to Si peak due to fixing sample on silicon wafer, and the EDX analysis proved the purity of the prepared AR-AgNPs. These results agreed well with previous reports (Ajitha et al., 2015; Yuan et al., 2017).

Fig. 1c shows XRD spectrum of synthesized AR-AgNPs, in which the Bragg reflections at $2\theta = 27.40°$, 31.81°, 37.85°, 45.86°, 68.87°, 76.51° and 85.91° correspond to (210), (122), (111), (200), (220), (311) and (222) lattice planes, respectively. These results indicated the face-centered cubic (FCC) structure of AR-AgNPs.

Fig. 1d shows the FTIR spectrum of AR-AgNPs. The band at 865 cm^{-1} could be from vibration of −CH stretching (Nayak et al., 2016). The peaks at 1010 cm^{-1} and 1061 cm^{-1} were assigned to the C−O stretching in phenolic compounds (Edison et al., 2016), while the band at 1334 cm^{-1} was attributed to O−H stretching of flavonoids (Joseph and Mathew, 2015). The appearance of the two peaks at 1581 cm^{-1} and 1731 cm^{-1} could represent the existence of amide I and II bands in proteins (Solomun et al., 2004; Sheny et al., 2011). The band at 2818 cm^{-1} could be the sign of C−H groups in aliphatic acids (Karthik et al., 2016). In addition, the wide peak at 3244 cm^{-1} indicated the OH group in phenolic compounds and alcohols (Liu et al., 2017).

Previous studies found that *A. rosea* was rich in galacturonic acid, glucuronic acid, rhamnose and galactose compounds (Ebrahiminezhad et al., 2017). *A. rosea* leaf extract contained high amounts of alkaloids, flavonoids and proteins (Ebrahiminezhad et al., 2017; Khoei et al., 2012), and carbohydrates like galacturonic acid, glucuronic acid, rhamnose and galactose compounds (Ebrahiminezhad et al., 2017). Various functional groups in these compounds could function as reducing agents to reduce the Ag^+ ions into AgNPs, and capping agents to stabilize the formed AR-AgNPs. Thus, the possible formation mechanism of the AR-AgNPs has been proposed and presented in Fig. S5.

3.3. C. vulgaris experiments

3.3.1. Toxic effects of AR-AgNPs, Ag^+ ions and coating agent on C. vulgaris

For perceiving toxicity of AR-AgNPs and their precursors (Ag^+ ions and coating agent) to algae biomass, their impacts during the exposure period i.e., 24, 48 and 72 h were investigated (Fig. 2). The algal biomass in the tested media were lower than that in control with different concentrations of AR-AgNPs and Ag^+ ions at the

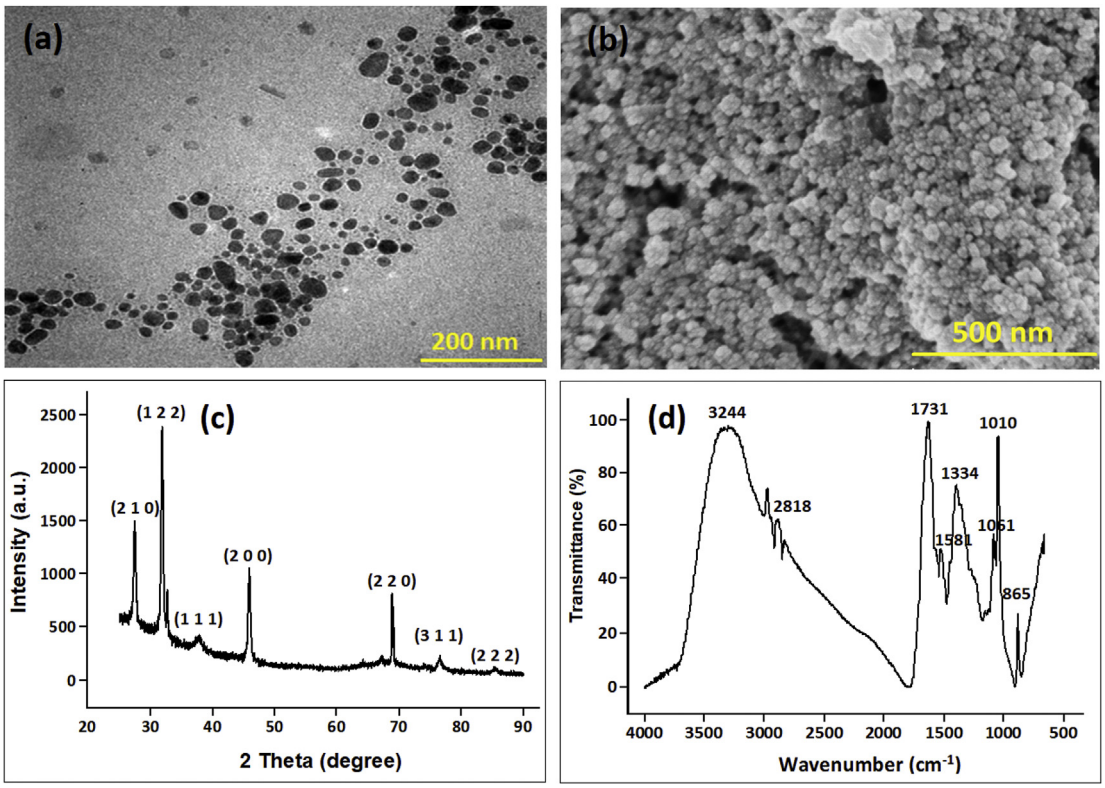

Fig. 1. TEM image (a), SEM image (b), XRD spectrum (c) and FTIR spectrum (d) of the synthesized AR-AgNPs. Synthesis conditions: $AgNO_3$ concentration, 1 mM; leaf extract/$AgNO_3$ = 1:60; reaction time, 7 h; temperature, 60 °C.

given interval time ($p < 0.05$). The greater reduction of algae biomass appeared at higher contents of AR-AgNPs and Ag^+ ions (50 μg/L) compared to the lower reduction at lower concentration of AR-AgNPs (Fig. 2a and b). This result suggested a dose-dependent effect of AR-AgNPs or Ag^+ ions on *C. vulgaris* biomass, which agreed with previous report on the toxicity of chemical AgNPs and Ag^+ ions on biomass changes of microalgae *D. salina* (Johari et al., 2018) and *M. aeruginosa* (Xiang et al., 2018). The biomass changes were not observed in the presence of the coating agent, indicating no toxicity to *C. vulgaris* (Fig. 2c, $p > 0.05$). It should be noted that the algae in Fig. 2c were exposed to different volumes of coating agents (*A. rosea* leaf extract) contained the corresponding AR-AgNPs suspensions, and the listed numbers (e.g., 5, 10, 20, 30, 40 and 50 μg/L) were just the concentrations of AR-AgNPs. This is the same as the following figures for the coating agent.

The relationship between concentrations of AR-AgNPs/Ag^+ ions and their effects on growth inhibition of *C. vulgaris* (after 72 h) were obtained by using the dose-response curves (Fig. S6). The 72 h-EC_{50} of AR-AgNPs to *C. vulgaris* biomass was 33.63 ± 2.10 μg/L, which was higher than 72 h-EC_{50} of Ag^+ ions (20.12 ± 1.55 μg/L), indicating the higher toxicity of Ag^+ ions than AR-AgNPs.

To further assess the toxicity of AR-AgNPs, Ag^+ ions and the coating agent to *C. vulgaris*, the total chlorophyll *a* contents of algae during the toxicity tests were determined (Fig. 2d–f). There were statistically significant difference among chlorophyll *a* contents in the control and media treated with different concentrations of AR-AgNPs or Ag^+ ions at the same exposure period (ANOVA, $p < 0.05$). The reduction of chlorophyll *a* contents increased with the increase of concentrations of AR-AgNPs and Ag^+ ions, which indicated the growth inhibition of AR-AgNPs and Ag^+ ions on algal growth. As with previous tests, there was no substantial differences of the chlorophyll *a* contents between the control and algae treated with the coating agents (Fig. 2f, ANOVA, $p > 0.05$), further indicating no toxicity of coating agent to algae cells.

Algae communities are important because they can generate oxygen and be as primary producer in aquatic ecosystems, thus AgNPs pollution may cause serious disturbances on algae functions or even the overall function of aqueous ecosystems (Oukarroum et al., 2012). Usually, the damage of NPs to multicellular organisms happens at their respiration system or skin, while unicellular organisms like microalga can be affected overall by NPs (Moreno-Garrido et al., 2015). Many mechanisms can explain the toxicity caused by AgNPs, including adhesion to membranes, increasing porosity of the cells, collapse of proton pumps, generation of ROS, degradation of lipopolysaccharide molecules, DNA damage, inhibition of DNA synthesis, inactivation of proteins and enzymes, and denaturation of ribosomes (Hu et al., 2018; Moreno-Garrido et al., 2015; Xiang et al., 2018).

3.3.2. Ag^+ ions release from AR-AgNPs to algal medium and their contribution to growth inhibition of *C. vulgaris*

In general, the toxicity of AgNPs may result from their particles directly or from the release of Ag^+ ions indirectly. Thus, it is important to determine the content of the released Ag^+ ions from AgNPs and its exact contribution to toxicity of AR-AgNPs to *C. vulgaris*. The existence of Ag^+ ions in algal medium might be from the presence of Ag^+ ions as precursor of biosynthesis process or the dissolution of AR-AgNPs, but the former one could be ignored because the biosynthesis yield was approximately 100%. The released Ag^+ ions from AR-AgNPs to *C. vulgaris* media at different exposure concentrations and different times were less than 1% of initial amounts of AR-AgNPs (Fig. S7), indicating the high stability of AR-AgNPs. The relationship between concentrations of Ag^+ ions (X axis) and algae growth inhibition (Y axis) was presented with the

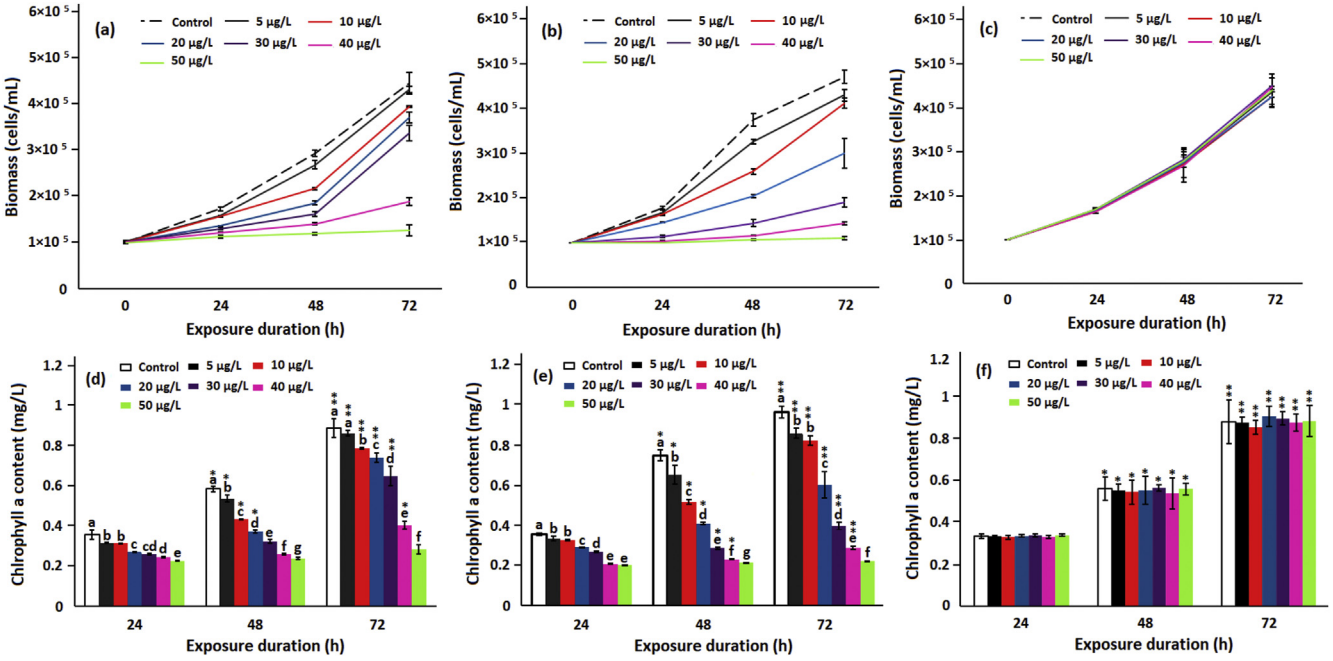

Fig. 2. The effects of varied concentrations of AR-AgNPs (a), Ag^+ ions (b) and coating agent (c) on biomass changes of algae *C. vulgaris* at different exposure durations. Changes in chlorophyll *a* content of *C. vulgaris* after exposure to different concentrations of AR-AgNPs (d), Ag^+ ions (e) and coating agent (f) at different time intervals. Letters represent significant differences among treatment groups within the same exposure period and asterisks display significant differences among different time intervals for the same concentration (one-way ANOVA with a post-hoc Duncan's test, $p < 0.05$).

dose-response equation in sigmoid curve (Fig. S6b), and indicated the insignificant contribution of released Ag^+ ions compared to the whole toxicity (less than 7%, Table S1).

3.3.3. Morphological changes of C. vulgaris after AR-AgNPs exposure

The morphological changes of *C. vulgaris* caused by AR-AgNPs were observed by using a light microscope with LCD display (Fig. S8). No algal cell aggregation was seen in the control group after 72 h exposure (Fig. S8a), while cellular aggregates formed and increased with increasing AR-AgNPs concentration (Figs. S8b–d). Extensive cellular aggregates were observed in cells exposed to 50 µg/L AR-AgNPs. These findings revealed that AR-AgNPs had direct toxicity to *C. vulgaris* cells by increasing cell aggregate formation. Such an effect on freshwater microalga *C. vulgaris* and marine microalga *Dunaliella tertiolecta* was also observed for chemical AgNPs (Oukarroum et al., 2012). This phenomenon can reduce algae access to light and absorption of required elements and nutrients from the aqueous medium, which inevitably inhibited algal growth (Oukarroum et al., 2012).

3.4. D. magna expriments

3.4.1. Toxic effects of AR-AgNPs, Ag^+ ions and coating agent on D. magna

To evaluate the toxicity of AR-AgNPs and Ag^+ ions towards *D. magna*, the dose-response curves under 24 and 48 h exposure were drawn (Fig. 3). No obvious change was observed in the percentages of living daphnids after exposure of *D. magna* to coating agent (Fig. S9), indicating no significant effect of coating agent on the mortality of *D. magna* (ANOVA, $p > 0.05$). However, after exposure of *D. magna* to AR-AgNPs and Ag^+ ions, mortality was observed and the higher the concentration, the greater the mortality rate (Fig. 3). The 48-h LC_{50} of AR-AgNPs and Ag^+ ions to daphnids were 1.86 ± 0.12 and 1.30 ± 0.07 µg/L, respectively, suggesting the higher toxicity of Ag^+ ions to *Daphnia* mortality than AR-AgNPs. These results are in agreement with the previous reports about the lower toxicity of chemical AgNPs than Ag^+ ions (Allen et al., 2010; Zhao and Wang, 2011). In addition, AR-AgNPs still had high toxicity to *D. magna,* probably indicates that the *D. magna* was vulnerable to AR-AgNPs.

The toxicity of AgNPs to aquatic organisms usually arisen from the release of free Ag^+ ions and themselves (Liu and Hurt, 2010; Asharani et al., 2008). The toxicity of Ag^+ ions to organisms might attribute to ion regulatory disturbance and competitive inhibition of potassium or sodium ion-dependent adenosine triphosphate (Na^+, K^+-ATPase) activity, which inhibited the *Daphnia*'s uptake of Na^+ (Bianchini et al., 2002). After penetrating into living cells, AgNPs can generate ROS and oxidative stress and cause negative effects such as membrane lipid peroxidation, mitochondrial damage, DNA damage, and consequently cell apoptosis (Choi et al., 2010; Lubick, 2008).

3.4.2. The release of Ag^+ ions from AR-AgNPs to Daphnia medium and their contribution to mortality of D. magna

The release of Ag^+ ions from AR-AgNPs to *D. magna* media occurred in all samples, and the amounts of Ag^+ ions after 24 and 48 h were less than 6% of the initial AR-AgNPs concentrations (Fig. S10). This indicates that AR-AgNPs were relatively stable in *D. magna* media. By using dose-response equation, the released Ag^+ ions from AR-AgNPs contributed 4.39–10.10% to *Daphnia* mortality after 48 h of exposure (Table S1), demonstrating the small impact of Ag^+ ions on *Daphnia* mortality. Similar result has been reported that the released Ag^+ ions from citrate-coated AgNPs contributed to the acute toxicity of *D. magna,* but the main cause of toxicity was AgNPs (Hu et al., 2018).

3.4.3. Uptake of AR-AgNPs to D. magna

After 48 h exposure of 1.5 µg/L AR-AgNPs, some brown pigments in the gill area and on the trunk limbs were observed under the

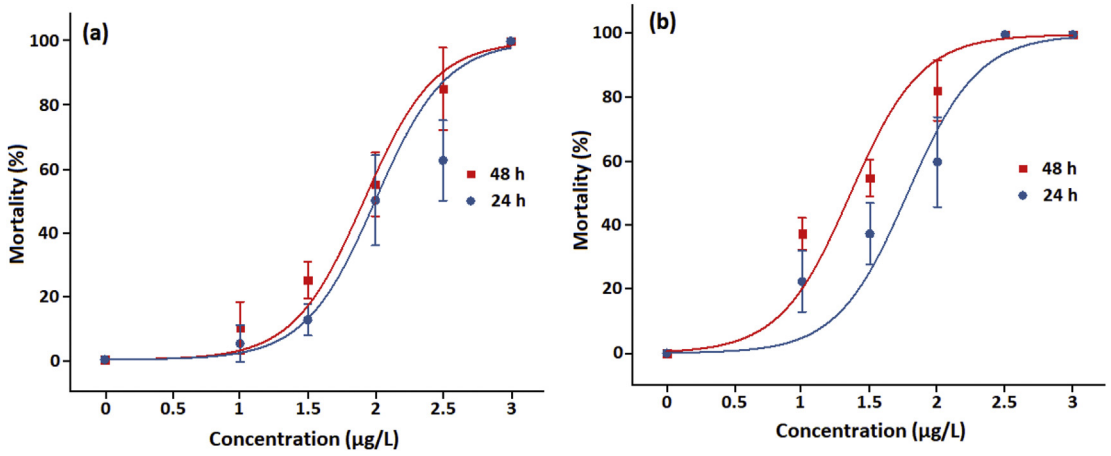

Fig. 3. Relationship between different concentrations of AR-AgNPs (a)/Ag^+ ions (b) and their effects on mortality (%) of *D. magna* after 24 and 48 h exposure based on dose-response curve.

light microscope, which was not seen in the control group (Fig. S11). This phenomenon was also observed when *D. magna* exposed to chemical AgNPs (Gaiser et al., 2011; Volker et al., 2013; Asghari et al., 2012). These pigments probably implied AR-AgNPs accumulation (Asghari et al., 2012). Although previous studies reported that AgNPs were mainly accumulated in *Daphnia* gut tract (Zhao and Wang, 2011; Asghari et al., 2012), this was not observed in this study probably due to the low concentration of AR-AgNPs (1.5 µg/L) that used. Other researchers also reported the uptake of AgNPs by daphnids from the test solutions (Roberts et al., 2007; Heinlaan et al., 2011). Given that *D. magna* locates at lower trophic levels and is food for other organisms at higher trophic levels, AR-AgNPs might be transferred from daphnids to higher organisms (Asghari et al., 2012). Change of storage lipids to lipid droplets under the *Daphnia* carapace caused by AR-AgNPs was another observed abnormality (Fig. S11c), these lipid droplets may cause negative effects on growth, regulate moulting and reproduction in *D. magna* (Fuertes et al., 2018). Appearance of lipid droplets was also reported when daphnids exposed to chemical AgNPs (Asghari et al., 2012).

3.5. *D. rerio* experiments

3.5.1. *Toxic effects of AR-AgNPs, Ag^+ ions and coating agent on D. rerio*

Fig. 4 shows the toxicity of AR-AgNPs and their precursors (Ag^+ ions and coating agent) towards *D. rerio*, suggesting that coating agent had no effect on *D. rerio* mortality ($p > 0.05$), whereas the mortality increased with time and the concentrations of AR-AgNPs and Ag^+ ions. Additionally, the 96-h LC_{50} values for AR-AgNPs and Ag^+ ions were 10.09 ± 0.05 and 4.74 ± 3.25, respectively, indicating the higher toxicity of Ag^+ ions than AR-AgNPs. During the initial phase of exposure, *D. rerio* showed the raised swimming activity, respiratory rate and efforts to escape from the glass beakers especially at higher AR-AgNPs concentrations (>15 µg/L) after 1 h of exposure. This suggested the toxic stress of AR-AgNPs on *D. rerio*.

The toxicity of Ag^+ ions and AgNPs might arise from their accumulation, penetration and gene alterations to target organs. Ag^+ ions were reported to be able to accumulate and bind to gill epithelium, thus fish gills were the primary target organs for Ag^+ ions in AgNPs, and the normally active uptake of Na^+ and Cl^- was thus inhibited (Wood et al., 1996; Ratte, 1999). NPs could penetrate different layer of skin (such as epithelium, epidermis and mitochondrion), gills, brain and liver, which would damage these organs and alter the gene expression (Lee et al., 2012).

As a Cholinesterase (ChEs) enzyme, AChE principally situated in the membrane of post-synaptic nervous cells and usually employed as a biomarker for neurotoxic studies (Behra et al., 2002; Payne et al., 1996). AChE can terminate neurotransmission by catalyzing the breakdown of acetylcholine (a neurotransmitter) into choline and acetate (Silman and Sussman, 2008). As toxic pollutants can change the AChE activity (Payne et al., 1996), the toxicity of AgNPs, Ag^+ ions and coating agent can be evaluated by AChE activity.

Fig. 5 presents the muscle and gill AChE activity of adult zebrafish after exposure to sub-lethal concentrations of AR-AgNPs (2 and 3 µg/L) and their precursors (Ag^+ ions and coating agent) at 0, 48 and 96 h. The results showed no difference in muscle AChE activity of zebrafish for AR-AgNPs, Ag^+ ions and coating agent (Fig. 5a–c) compared to the controls (ANOVA, $p > 0.05$). This indicated that AR-AgNPs and their precursors were non-toxic to zebrafish muscle. Although previous study reported the reduction of AChE activity in zebrafish muscle after exposure to chemical AgNPs (Katuli et al., 2014), this different result might be caused by the different exposure time with 7 days vs 4 days.

In contrast to muscle AChE activity, the gill AChE activity of zebrafish decreased when exposed to AR-AgNPs (Fig. 5d) and Ag^+ ions (Fig. 5e) in compare with the controls (ANOVA, $p < 0.05$), indicating the adverse effects of AgNPs and Ag^+ ions on fish gill. No significant change of AChE activity was observed when exposed to coating agent, ($p > 0.05$, Fig. 5f), and indicated the safety of the coating agent.

AChE plays an important role in neural pathways of fishes and muscular development, and the decreased AChE activity may lower fish survival rate (Behra et al., 2002; Fulton and Key, 2001). In addition, the physiological functions of AChE included food and feeding, spatial distribution pattern, social interactions, locomotor capacity, prey location and predator evasion (Bradbury et al., 2008). Hence, the results above indicated that the exposure of zebrafish to AR-AgNPs and Ag^+ ions would lead to the inhibition of AChE activity and further cause physiological and morphological abnormalities.

3.5.2. *Role of Ag^+ ions released from AR-AgNPs in D. rerio mortality*

Unlike the media of algae and daphnids, the fish medium renewed each 24 h based on OECD 203 guideline. Therefore, the amounts of free Ag^+ ions in fish media were measured each 24 h before changing of water. It was found that the media with 20 and 25 µg/L of AR-AgNPs released less than 0.3% of free Ag^+ ions based on initial concentrations. While other concentrations released too little Ag^+ ions to be detected by ICP-MS. This suggested the high

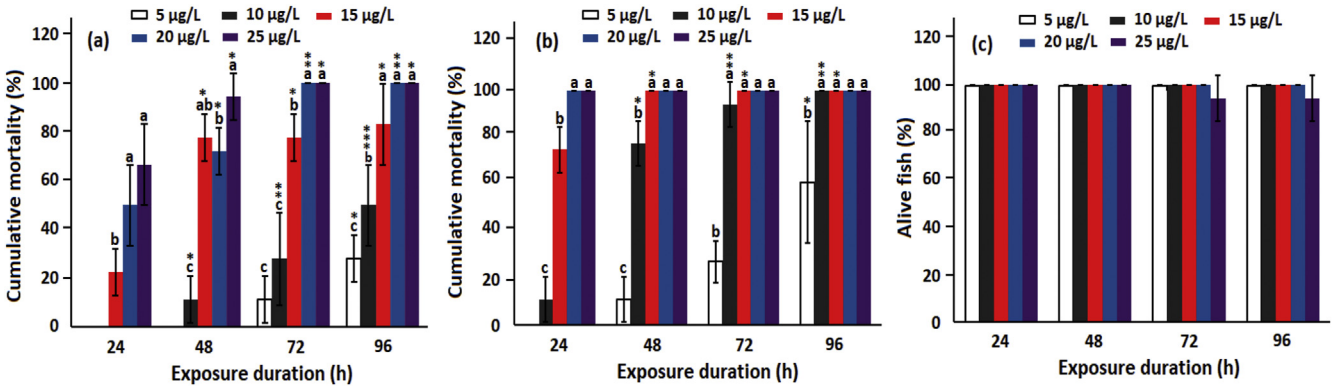

Fig. 4. Toxicity of different concentrations of AR-AgNPs (a) and Ag^+ ions (b) to zebrafish mortality at different exposure times, and the effect of coating agent (c) on zebrafish survival at different time intervals. Letters denote significant differences among treatment groups within the same exposure period and asterisks indicate significant differences among different time intervals for the same concentration (one-way ANOVA with a post-hoc Duncan's test, $p < 0.05$).

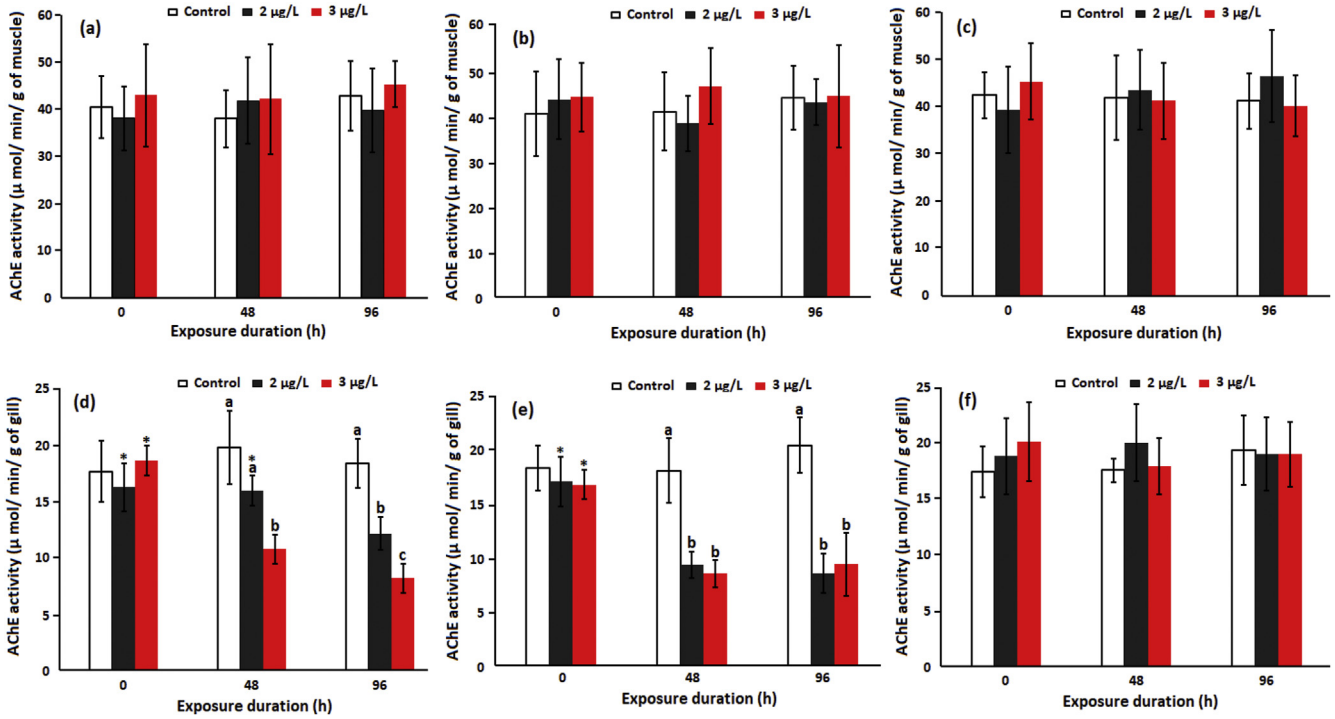

Fig. 5. Muscle AChE activity of zebrafish after exposure to sub-lethal concentrations (2 and 3 µg/L) of AR-AgNPs (a) and their precursors (Ag^+ ions (b) and coating agent (c)). The changes of gill AChE activity of zebrafish exposed to AR-AgNPs (d), Ag^+ ions (e) and coating agent (f) at 0, 48 and 96 h. Letters show significant differences among treatment groups within the same exposure period and asterisks display significant differences among different time intervals for the same concentration (one-way ANOVA with a post-hoc Duncan's test, $p < 0.05$).

stability of AR-AgNPs in fish medium and the little even no contribution of free Ag^+ ions to fish acute toxicity. This agreed well with previous report that AgNPs were lethal to zebrafish (Bilberg et al., 2012).

3.5.3. *Abnormalities of D. rerio exposed to AR-AgNPs*

After 24 h of acute toxicity tests and the removal of dead zebrafish from media containing AR-AgNPs, two clear abnormalities were observed for the dead zebrafish. These abnormalities included ascites (accumulation of fluid in the abdomen) and color change (fading color) (Fig. S12), which were more severe for fish exposed to 25 µg/L of AR-AgNPs. This further indicated the adverse effects of AR-AgNPs on zebrafish growth.

4. Conclusions

Many studies have explored the toxic effects of physiochemically synthesized AgNPs to organisms. However, the toxicity and negative effects of biosynthesized AgNPs remain unclear, particularly in aquatic food chains. Herein, facile, cost effective and eco-friendly AR-AgNPs were synthesized by the reaction of silver nitrate with *A. rosea* leaf extract, and their potential toxicity towards organisms in aquatic food chain was investigated. With the increase of exposure dose, the biomass of *C. vulgaris* decreased with the occurrence of photosynthetic pigments, the mortality of *D. magna* and *D. rerio* increased, and gill AChE activity of *D. rerio* was inhibited. This indicated that the biosynthesized AgNPs could exert

toxic effects to numerous organisms at different trophic levels of aquatic ecosystems. Because this study referred to conventional OECD test methods, the roles of important parameters like pH, dissolved organic carbon (DOC), water hardness, cations (Ca^{2+}, Mg^{2+} and Na^{+}), sulfides and chlorides, which strongly affect the physio-chemical behaviors and toxicity of NPs (Kennedy et al., 2012) should be investigated in the future studies. Moreover, the toxicity of AgNPs synthesized using other plants or other biological methods towards other food chains/webs should be further studied.

Declaration of competing interest

The authors declare no competing interests.

The authors declare that they have no known competing financial interests or personal relationships that could have appeared to influence the work reported in this paper.

CRediT authorship contribution statement

Mehdi Khoshnamvand: Conceptualization, Methodology, Writing - original draft. **Zhineng Hao:** Methodology, Writing - review & editing. **Oluniyi O. Fadare:** Methodology. **Parichehr Hanachi:** Software, Validation. **Yongsheng Chen:** Writing - review & editing. **Jingfu Liu:** Supervision, Writing - review & editing.

Acknowledgments

Financial support for this work was given by the National Natural Science Foundation of China (21620102008). The authors would like to thank from Professor Wan Bin for using his fish laboratory. M.K appreciates the support of CAS-TWAS President's Fellowship for his Ph.D study.

Appendix A. Supplementary data

Supplementary data to this article can be found online at https://doi.org/10.1016/j.chemosphere.2020.127346.

References

Ajitha, B., Reddy, Y.A.K., Reddy, P.S., 2015. Green synthesis and characterization of silver nanoparticles using *Lantana camara* leaf extract. Mater. Sci. Eng. C 49, 373–381.

Ali, M.S., Anuradha, V., Yogananth, N., Krishnakumar, S., 2019. Heart and liver regeneration in zebrafish using silver nanoparticle synthesized from *Turbinaria conoides* – in vivo. Biocatal. Agric. Biotechnol. 17, 104–109.

Allen, H.J., Impellitteri, C.A., Macke, D.A., Heckman, J.L., Poynton, H.C., Lazorchak, J.M., Govindaswamy, S., Roose, L.D., Nadagouda, M.N., 2010. Effects from filtration, capping agents, and presence/absence of food on the toxicity of silver nanoparticles to *Daphnia magna*. Environ. Toxicol. Chem. 29 (12), 2742–2750.

Asghari, S., Johari, S.A., Lee, J.H., Kim, Y.S., Jeon, Y.B., Choi, H.J., Moon, M.C., Yu, J.Y., 2012. Toxicity of various silver nanoparticles compared to silver ions in *Daphnia magna*. J. Nanobiotechnol. 10, 14.

Asharani, P.V., Wu, Y.L., Gong, Z., Valiyaveettil, S., 2008. Toxicity of silver nanoparticles in zebra fish models. Nanotechnology 19, 251–262.

Behra, M., Cousin, X., Bertrand, C., Vonesch, J.L., Biellmann, D., Chatonnet, A., Strahle, U., 2002. Acetylcholinesterase is required for neuronal and muscular development in the zebrafish embryo. Nat. Neurosci. 5, 111–118.

Bianchini, A., Grosell, M., Gregory, S.M., Wood, C.M., 2002. Acute silver toxicity in aquatic animals is a function of sodium uptake rate. Environ. Sci. Technol. 36 (8), 1763–1766.

Bilberg, K., Hovgaard, M.B., Besenbacher, F., Baatrup, E., 2012. In vivo toxicity of silver nanoparticles and silver ions in zebrafish (*Danio rerio*). J. Toxicol. 2012, 293784. https://doi.org/10.1155/2012/293784.

Bradbury, S.P., Carlson, R.W., Henry, T.R., Padilla, S., Cowden, J., 2008. Toxic responses of the fish nervous system. In: Di Giulio, R.T., Hinton, D.E. (Eds.), The Toxicology of Fishes. CRC Press-Taylor & Francis Group, Boca Raton, FL, pp. 417–455.

Choi, J.E., Kim, S., Ahn, J.H., Youn, P., Kang, J.S., Park, K., Yi, J., Ryu, D.Y., 2010. Induction of oxidative stress and apoptosis by silver nanoparticles in the liver of adult zebrafish. Aquat. Toxicol. 100 (2), 151–159.

Ebrahiminezhad, A., Barzegar, Y., Ghasemi, Y., Berenjian, A., 2017. Green synthesis and characterization of silver nanoparticles using *Alcea rosea* flower extract as a new generation of antimicrobials. Chem. Ind. Chem. Eng. Q. 23 (1), 31–37.

Edison, T.N.J.I., Lee, Y.R., Sethuraman, M.G., 2016. Green synthesis of silver nanoparticles using *Terminalia cuneata* and its catalytic action in reduction of direct yellow-12 dye. Spectrochim. Acta A 161, 122–129.

Fuertes, I., Jordão, R., Casas, F., Barata, C., 2018. Allocation of glycerolipids and glycerophospholipids from adults to eggs in *Daphnia magna*: perturbations by compounds that enhance lipid droplet accumulation. Environ. Pollut. 242, 1702–1710.

Fulton, M.H., Key, P.B., 2001. Acetylcholinesterase inhibition in estuarine fish and invertebrates as an indicator of organophosphorus insecticide exposure and effects. Environ. Toxicol. Chem. 20 (1), 37–45.

Gaiser, B.K., Biswas, A., Rosenkranz, P., Jepson, M.A., Lead, J.R., Stone, V., Tyler, C.R., Fernandes, T.F., 2011. Effects of silver and cerium dioxide micro- and nano-sized particles on *Daphnia magna*. J. Environ. Monit. 13 (5), 1227–1235.

He, X., Aker, W.G., Fu, P.P., Hwang, H.M., 2015. Toxicity of engineered metal oxide nanomaterials mediated by nano–bio–eco–interactions: a review and perspective. Environ. Sci. Nano. 2, 564–582.

He, J., Wang, D., Zhou, D., 2019. Transport and retention of silver nanoparticles in soil: effects of input concentration, particle size and surface coating. Sci. Total Environ. 648, 102–108.

Heinlaan, M., Kahru, A., Kasemets, K., Arbeille, B., Prensier, G., Dubourguier, H.C., 2011. Changes in the *Daphnia magna* midgut upon ingestion of copper oxide nanoparticles: a transmission electron microscopy study. Water Res. 45 (1), 179–190.

Howe, K., Clark, M.D., Torroja, C.F., et al., 2013. The zebrafish reference genome sequence and its relationship to the human genome. Nature 496, 498–503.

Hu, P., Zhang, X., Li, Y., Pichan, C., Chen, Z., 2018. Molecular interactions between silver nanoparticles and model cell membranes. Top. Catal. 61 (9–11), 1148–1162.

Jang, G.H., Hwang, M.P., Kim, S.Y., 2014. A systematic in-vivo toxicity evaluation of nanophosphor particles via zebrafish models. Biomaterials 35, 440–449.

Johari, S.A., Sarkheil, M., Tayemeh, M.B., Veisi, S., 2018. Influence of salinity on the toxicity of silver nanoparticles (AgNPs) and silver nitrate ($AgNO_3$) in halophilic microalgae, *Dunaliella salina*. Chemosphere 209, 156–162.

Joseph, S., Mathew, B., 2015. Microwave-assisted green synthesis of silver nanoparticles and the study on catalytic activity in the degradation of dyes. J. Mol. Liq. 204, 184–191.

Karthik, R., Chen, S.M., Elangovan, A., Muthukrishnan, P., Shanmugam, R., Lou, B.S., 2016. Phyto mediated biogenic synthesis of gold nanoparticles using *Cerasus serrulata* and its utility in detecting hydrazine, microbial activity and DFT studies. J. Colloid Interface Sci. 468, 163–175.

Katuli, K.K., Massarsky, A., Hadadi, A., Pourmehran, Z., 2014. Silver nanoparticles inhibit the gill Na^{+}/K^{+}-ATPase and erythrocyte AChE activities and induce the stress response in adult zebrafish (*Danio rerio*). Ecotoxicol. Environ. Saf. 106, 173–180.

Kennedy, A.J., Chappell, M.A., Bednar, A.J., Ryan, A.C., Laird, J.G., Stanley, J.K., Steevens, J.A., 2012. Impact of organic carbon on the stability and toxicity of fresh and stored silver nanoparticles. Environ. Sci. Technol. 46 (19), 10772–10780.

Khoei, S., Azarian, M., Khoei, S., 2012. Effect of hyperthermia and triblock copolymeric nanoparticles as quercetin carrier on DU145 prostate cancer cells. Curr. Nanosci. 8 (5), 690–696.

Khoshnamvand, M., Ashtiani, S., Chen, Y., Liu, J., 2020a. Impacts of organic matter on the toxicity of biosynthesized silver nanoparticles to green microalgae *Chlorella vulgaris*. Environ. Res. 185, 109433.

Khoshnamvand, M., Ashtiani, S., Huo, C., Saebb, S.P., Liu, J.F., 2019a. Use of *Alcea rosea* leaf extract for biomimetic synthesis of gold nanoparticles with innate free radical scavenging and catalytic activities. J. Mol. Struct. 1179, 749–755.

Khoshnamvand, M., Ashtiani, S., Liu, J., 2020b. Acute toxicity of gold nanoparticles synthesized from alga *Saccharina japonica* towards *Daphnia* magna. Environ. Sci. Pollut. Res. 27, 22120–22126.

Khoshnamvand, M., Huo, C., Liu, J., 2019b. Silver nanoparticles synthesized using *Allium ampeloprasum* L. leaf extract: characterization and performance in catalytic reduction of 4-nitrophenol and antioxidant activity. J. Mol. Struct. 1175, 90–96.

Lee, B., Duong, C.N., Cho, J., Lee, J., Kim, K., Seo, Y., Kim, P., Choi, K., Yoon, J., 2012. Toxicity of citrate-capped silver nanoparticles in common carp (*Cyprinus carpio*). J. Biomed. Biotechnol. 262670. https://doi.org/10.1155/2012/262670.

Liu, J., Hurt, R.H., 2010. Ion release kinetics and particle persistence in aqueous nano-silver colloids. Environ. Sci. Technol. 44 (6), 2169–2175.

Liu, H., Lian, T., Liu, Y., Hong, Y., Sun, D., Li, Q., 2017. Plant-mediated synthesis of Au nanoparticles: separation and identification of active biomolecule in the water extract of *Cacumen Platycladi*. Ind. Eng. Chem. Res. 56, 5262–5270.

Lubick, N., 2008. Nanosilver toxicity: ions, nanoparticles – or both? Environ. Sci. Technol. 42, 8617.

Manzo, L., Castoldi, A.F., Coccini, T., Prockop, L.D., 2001. Assessing effects of neurotoxic pollutants by biochemical markers. Environ. Res. 85 (1), 31–36.

Moreno-Garrido, I., Perez, S., Blasco, J., 2015. Toxicity of silver and gold nanoparticles on marine microalgae. Mar. Environ. Res. 111, 60–73.

Mulenos, M.R., Liu, J., Lujan, H., Guo, B., Lichtfouse, E., Sharma, V.K., Sayes, C.M., 2020. Copper, silver, and titania nanoparticles do not release ions under anoxic conditions and release only minute ion levels under oxic conditions in water:

evidence for the low toxicity of nanoparticles. Environ. Chem. Lett. https://doi.org/10.1007/s10311-020-00985-z.
Nayak, D., Ashe, S., Rauta, P.R., Kumari, M., Nayak, B., 2016. Bark extract mediated green synthesis of silver nanoparticles: evaluation of antimicrobial activity and antiproliferative response against osteosarcoma. Mater. Sci. Eng. C 58, 44–52.
Nie, X., Zhu, K., Zhao, S., Dai, Y., Tian, H., Sharma, V.K., Jia, H., 2020. Interaction of Ag^{+} with soil organic matter: elucidating the formation of silver nanoparticles. Chemosphere 243, 25413.
OECD, 2011. OECD Guidelines for the Testing of Chemicals, Section 2: Freshwater Alga and Cyanobacteria Growth Inhibition Test. Test No. 201. Organisation for Economic Co-Operation and Development, Paris, France.
OECD, 2004. OECD Guidelines for the Testing of Chemicals: *Daphnia sp*., Acute Immobilization Test. Test No. 202. Organization for Economic Cooperation and Development, Paris, France.
OECD, 1992. Fish Acute Toxicity Test. Test No. 203. OECD Publishing.
Oukarroum, A., Bras, S., Perreault, F., Popovic, R., 2012. Inhibitory effects of silver nanoparticles in two green algae, *Chlorella vulgaris* and *Dunaliella tertiolecta*. Ecotoxicol. Environ. Saf. 78, 80–85.
Payne, J.F., Mathieu, A., Melvin, W., Fancey, L.L., 1996. Acetylcholinesterase, an old biomarker with a new future? Field trials in association with two urban rivers and a paper mill in Newfoundland. Mar. Pollut. Bull. 32 (2), 225–231.
Persoone, G., Baudo, R., Cotman, M., et al., 2009. Review on the acute *Daphnia magna* toxicity test-evaluation of the sensitivity and the precision of assays performed with organisms from laboratory cultures or hatched from dormant eggs. Knowl. Manag. Aquat. Ecosyst. 393, 1. https://doi.org/10.1051/kmae/2009012.
Rani, P.U., Rajasekharreddy, P., 2011. Green synthesis of silver-protein (core–shell) nanoparticles using *Piper betle* L. leaf extract and its ecotoxicological studies on *Daphnia magna*. Colloids Surf., A 389 (1–3), 188–194.
Ratte, H.T., 1999. Bioaccumulation and toxicity of silver compounds: a review. Environ. Toxicol. Chem. 18 (1), 89–108.
Roberts, A.P., Mount, A.S., Seda, B., Souther, J., Qiao, R., Lin, S., Ke, P.C., Rao, A.M., Klaine, S.J., 2007. In vivo biomodification of lipid-coated carbon nanotubes by *Daphnia magna*. Environ. Sci. Technol. 41 (8), 3025–3029.
Sakka, Y., Skjolding, L.M., Mackevica, A., Filser, J., Baun, A., 2016. Behavior and chronic toxicity of two differently stabilized silver nanoparticles to *Daphnia magna*. Aquat. Toxicol. 177, 526–535.
Sanchez, G.R., Castilla, C.L., Gomez, N.B., Garcia, A., Marcos, R., Carmona, E.R., 2016. Leaf extract from the endemic plant *Peumus boldus* as an effective bioproduct for the green synthesis of silver nanoparticles. Mater. Lett. 183, 255–260.
Shankar, P.D., Shobana, S., Karuppusamy, I., Pugazhendhi, A., Ramkumar, V.S., Arvindnarayan, S., Kumar, G., 2016. A review on the biosynthesis of metallic nanoparticles (gold and silver) using bio-components of microalgae: formation mechanism and applications. Enzym. Microb. Technol. 95, 28–44.
Sharma, V.K., Filip, J., Zborilb, R., Varma, R.S., 2015. Natural inorganic nanoparticles – formation, fate, and toxicity in the environment. Chem. Soc. Rev. 44, 8410.
Shen, M.H., Zhou, X.X., Yang, X.Y., Chao, J.B., Liu, R., Liu, J.F., 2015. Exposure Medium: key in identifying free Ag^{+} as the exclusive species of silver nanoparticles with acute toxicity to *Daphnia magna*. Sci. Rep. 5, 9674.
Sheny, D.S., Mathew, J., Philip, D., 2011. Phytosynthesis of Au, Ag and Au–Ag bimetallic nanoparticles using aqueous extract and dried leaf of *Anacardium occidentale*. Spectrochim. Acta A 79, 254–262.
Silman, I., Sussman, J.L., 2008. Acetylcholinesterase: how is structure related to function? Chem. Biol. Interact. 175, 3–10.
Solomun, T., Schimanski, A., Sturm, H., Illenberger, E., 2004. Reactions of amide group with fluorine as revealed with surface analytics. Chem. Phys. Lett. 387 (4–6), 312–316.
Volker, C., Boedicker, C., Daubenthaler, J., Oetken, M., Oehlmann, J., 2013. Comparative toxicity assessment of nanosilver on three daphnia species in acute, chronic and multi-generation experiments. PloS One 8 (10), e75026.
Weinberg, H., Galyean, A., Leopold, M., 2011. Evaluating engineered nanoparticles in natural waters. Trends Anal. Chem. 30, 72–83.
Wood, C.M., Hogstrand, C., Galvez, F., Munger, R.S., 1996. The physiology of waterborne silver toxicity in freshwater rainbow trout (*Oncorhynchus mykiss*) 1. The effects of ionic Ag^{+}. Aquat. Toxicol. 35 (2), 93–109.
Xiang, L., Fang, J., Cheng, H., 2018. Toxicity of silver nanoparticles to green algae *M. aeruginosa* and alleviation by organic matter. Environ. Monit. Assess. 190, 667.
Yu, S.J., Yin, Y.G., Liu, J.F., 2013. Silver nanoparticles in the environment. Environ. Sci. Process Impacts 15, 78–92.
Yuan, C.G., Huo, C., Gui, B., Liu, P., Zhang, C., 2017. Green synthesis of silver nanoparticles using *Chenopodium aristatum* L. stem extract and their catalytic/antibacterial activities. J. Cluster Sci. 28 (3), 1319–1333.
Zhao, C.M., Wang, W.X., 2011. Comparison of acute and chronic toxicity of silver nanoparticles and silver nitrate to *Daphnia magna*. Environ. Toxicol. Chem. 30 (4), 885–892.